

Exciting the Goldstone Modes of a Supersolid Spin–Orbit-Coupled Bose Gas

Kevin T. Geier,^{1,2,*} Giovanni I. Martone,³ Philipp Hauke,¹ and Sandro Stringari¹

¹*INO-CNR BEC Center and Dipartimento di Fisica, Università di Trento, 38123 Povo, Italy*

²*Institute for Theoretical Physics, Ruprecht-Karls-Universität Heidelberg, Philosophenweg 16, 69120 Heidelberg, Germany*

³*Laboratoire Kastler Brossel, Sorbonne Université, CNRS,*

ENS-PSL Research University, Collège de France; 4 Place Jussieu, 75005 Paris, France

(Dated: September 21, 2021)

Supersolidity is deeply connected with the emergence of Goldstone modes, reflecting the spontaneous breaking of both phase and translational symmetry. Here, we propose accessible signatures of these modes in harmonically trapped spin–orbit-coupled Bose–Einstein condensates, where supersolidity appears in the form of stripes. By suddenly changing the trapping frequency, an axial breathing oscillation is generated, whose behavior changes drastically at the critical Raman coupling. Above the transition, a single mode of hybridized density and spin nature is excited, while below it, we predict a beating effect signaling the excitation of a Goldstone spin-dipole mode. We further provide evidence for the Goldstone mode associated with the translational motion of stripes. Our results open up new perspectives for probing supersolid properties in experimentally relevant configurations with both symmetric as well as highly asymmetric intraspecies interactions.

Supersolidity is an exotic state of matter characterized by the simultaneous spontaneous breaking of $U(1)$ symmetry, yielding superfluidity, and of translational invariance, yielding crystallization [1–3]. In the past, this state of matter has attracted considerable attention in the context of solid helium, where the experimental efforts to reveal the effects of superfluidity, however, have not been conclusive [4, 5]. More recently, a renewed interest has emerged in the context of ultracold atomic gases, and experimental evidence of typical supersolid features has been reported in Bose–Einstein condensates inside optical resonators [6], spin–orbit-coupled configurations [7, 8], and in cold gases interacting with long-range dipole forces [9–11]. An important property of supersolidity with respect to ordinary superfluids is the appearance of additional gapless (Goldstone) modes in the excitation spectrum, resulting from the broken translational symmetry [2, 12–21]. While these modes have already been the object of first experimental investigation inside optical resonators [22] and in harmonically trapped dipolar gases [23–26], so far no experimental observation has been reported in spin–orbit-coupled configurations.

An important motivation behind the present Letter is to better understand the significance of the spin degree of freedom for the excitation mechanisms of the Goldstone modes in the supersolid phase. Focusing on a harmonically trapped spin–orbit-coupled Bose–Einstein-condensed gas, we identify a characteristic beating effect that allows for the observation of a Goldstone excitation of spin nature, in analogy to a similar procedure followed in dipolar supersolids [23]. Moreover, we show that the locking of the polarization after a uniform spin perturbation provides evidence for the Goldstone mode associated with the rigid translation of the stripes [24].

Spin–orbit-coupled Bose–Einstein condensates are known to exhibit an intriguing variety of quantum phases, which are obtained by tuning the experimen-

tally controllable Raman coupling, responsible for coherence between atoms occupying two different hyperfine states [27–29]. Spin–orbit coupling gives rise to an effective single-particle Hamiltonian of the form [30]

$$H_{\text{SP}} = \frac{1}{2m} (\mathbf{p} - \hbar \mathbf{k}_0 \sigma_z)^2 + \frac{\Omega}{2} \sigma_x + \frac{\delta}{2} \sigma_z + V(\mathbf{r}), \quad (1)$$

where m is the atomic mass, and σ_x and σ_z are Pauli matrices. The spin–orbit term, fixed by the momentum transfer $\hbar \mathbf{k}_0 = \hbar k_0 \hat{\mathbf{e}}_x$ between two intersecting laser fields generating the Raman coupling with strength Ω and effective detuning δ , is at the origin of non-trivial many-body effects which deeply differ from the ones caused by simple coherent coupling with negligible momentum transfer, such as radio frequency or microwave coupling. We are, in particular, interested in the observability of the Goldstone modes in the presence of a harmonic trapping potential $V(\mathbf{r}) = m(\omega_x^2 x^2 + \omega_y^2 y^2 + \omega_z^2 z^2)/2$, with frequencies ω_i and associated oscillator lengths $a_i = \sqrt{\hbar/m\omega_i}$, $i = x, y, z$.

In what follows, we assume that the two-body interaction between the atoms is described within the usual mean-field Gross–Pitaevskii theory of quantum mixtures [31]. Then, writing the order parameter in the spinor form $\Psi = (\Psi_\uparrow, \Psi_\downarrow)^T$ with the wave functions Ψ_\uparrow and Ψ_\downarrow describing the relevant hyperfine states, the energy of the system is

$$E = \int d\mathbf{r} \left(\Psi^\dagger H_{\text{SP}} \Psi + \frac{g_{\text{nn}} n^2}{2} + \frac{g_{\text{ss}} s_z^2}{2} + g_{\text{ns}} n s_z \right). \quad (2)$$

Here, $g_{\text{nn}} = (g_{\uparrow\uparrow} + g_{\downarrow\downarrow} + 2g_{\uparrow\downarrow})/4$, $g_{\text{ss}} = (g_{\uparrow\uparrow} + g_{\downarrow\downarrow} - 2g_{\uparrow\downarrow})/4$, and $g_{\text{ns}} = (g_{\uparrow\uparrow} - g_{\downarrow\downarrow})/4$ denote, respectively, the density–density, spin–spin, and density–spin interaction parameters, fixed by proper combinations of the coupling constants $g_{ij} = 4\pi\hbar^2 a_{ij}/m$, where a_{ij} are the respective scattering lengths with $i, j \in \{\uparrow, \downarrow\}$. The particle density and the spin density entering Eq. (2) are defined, respectively, as $n(\mathbf{r}) = |\Psi_\uparrow(\mathbf{r})|^2 + |\Psi_\downarrow(\mathbf{r})|^2$ and

$s_z(\mathbf{r}) = |\Psi_\uparrow(\mathbf{r})|^2 - |\Psi_\downarrow(\mathbf{r})|^2$, the former being normalized to the total particle number $N = \int d\mathbf{r} n(\mathbf{r})$. Averages of an observable O are defined as $\langle O \rangle = \int d\mathbf{r} \Psi^\dagger O \Psi / N$, or, with respect to an individual spin component i , as $\langle O \rangle_i = \int d\mathbf{r} \Psi_i^* O \Psi_i / \int d\mathbf{r} |\Psi_i|^2$. Depending on the values of the parameters entering the energy functional (2), the ground state of the system can be either in the single-minimum, plane-wave, or stripe phase, hereafter also called the supersolid phase (see, e.g., Ref. [32]). The use of the mean-field picture is justified by the fact that the quantum depletion of the condensate in these dilute quantum mixtures is a negligible effect (on the order of 1%), even in the presence of spin-orbit coupling [33, 34].

In order to explore the nature of the elementary excitations, we numerically solve the coupled time-dependent Gross-Pitaevskii equations, directly derivable from the variation of the action $S = \int dt E[\Psi_\uparrow, \Psi_\downarrow] - i\hbar \int dt d\mathbf{r} (\Psi_\uparrow^* \partial_t \Psi_\uparrow + \Psi_\downarrow^* \partial_t \Psi_\downarrow)$ with respect to Ψ_\uparrow^* and Ψ_\downarrow^* . More specifically, we compute the ground state of the system in the presence of a static perturbation of density or spin nature by means of a non-linear conjugate gradient method [35]. At time $t = 0$, the perturbation is suddenly removed, and the quenched system is evolved in time using a time-splitting Fourier pseudospectral method [36]. The frequencies of the induced collective oscillations are extracted from sinusoidal fits to the time traces of the relevant observables.

We first investigate the case of symmetric intraspecies interactions, while the effects of strong asymmetries in the couplings are explored toward the end of this Letter. The majority of previous works focuses on symmetric configurations, as it is well realized, for instance, by ^{87}Rb [30]. For our purposes, we choose a configuration close to ^{87}Rb with $a_{\uparrow\uparrow} = a_{\downarrow\downarrow} = 100 a_0$, where a_0 is the Bohr radius. Naturally, ^{87}Rb is characterized by a value of $g_{\uparrow\downarrow}$ very close to $g_{\uparrow\uparrow}$ and $g_{\downarrow\downarrow}$, yielding $g_{\text{ss}} \approx 0$, and hence a small value of the critical Raman coupling $\Omega_{\text{cr}} = 4E_r \sqrt{2g_{\text{ss}}/(g_{\text{nn}} + 2g_{\text{ss}})}$ for the transition to the supersolid phase [37, 38], where $E_r = \hbar^2 k_0^2 / 2m$ is the recoil energy. Increasing the value of Ω_{cr} is desirable to limit the effects of magnetic fluctuations and to observe visible consequences of the presence of stripes. To this end, we consider configurations characterized by an effective reduction of the coupling constant $g_{\uparrow\downarrow}$. This may be achieved by reducing the spatial overlap between the wave functions of the two spin components, for instance, with the help of a spin-dependent trapping potential separating the two components [39, 40], or using pseudo-spin orbital states in a superlattice potential [7]. Here, we follow the former approach, using a quasi-2D harmonic trap with frequencies $(\omega_x, \omega_y, \omega_z) = 2\pi \times (50, 200, 2500)$ Hz, where the two spin components are separated along the z direction such that the effective 2D interspecies coupling becomes $\tilde{g}_{\uparrow\downarrow} = 0.6 \tilde{g}_{\uparrow\uparrow}$ with $\tilde{g}_{\uparrow\uparrow} = g_{\uparrow\uparrow} / \sqrt{2\pi} a_z = \tilde{g}_{\downarrow\downarrow}$ [39]. The reported Raman coupling Ω corresponds to an effective coupling, accounting for the reduced spa-

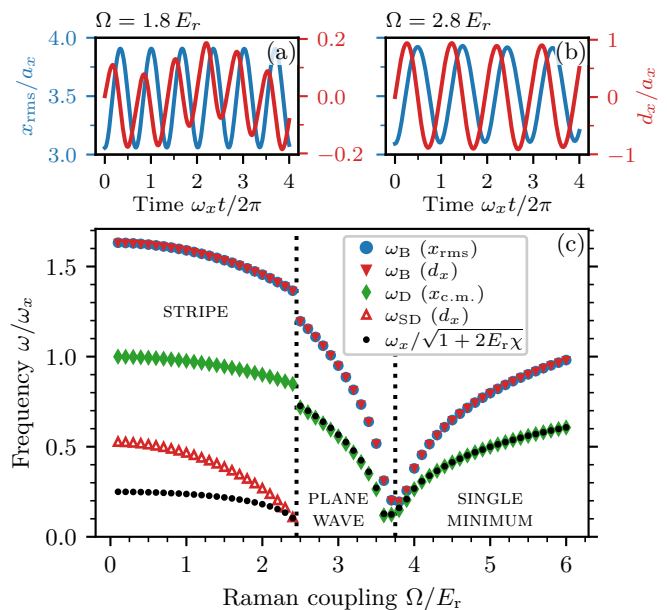


Figure 1. Collective modes for symmetric intraspecies interactions. (a),(b) Oscillations of the observables $x_{\text{rms}} = \sqrt{\langle x^2 \rangle}$ and $d_x = \langle x \rangle_\uparrow - \langle x \rangle_\downarrow$ after suddenly removing the perturbation $H_{\text{pert}} = \lambda m \omega_x^2 x^2$ with $\lambda = 0.2$. In the stripe phase (a), a clear beating of two frequencies $\omega_B \approx 1.49 \omega_x$ and $\omega_{\text{SD}} \approx 0.32 \omega_x$ is visible in the observable d_x , which is absent in the plane-wave phase (b), where d_x oscillates only at a single frequency $\omega_B \approx 1.02 \omega_x$. (c) Dispersion $\omega(\Omega)$ of the breathing mode (B), the spin-dipole mode (SD), and the center-of-mass (dipole) mode (D), calculated for $\lambda \ll 1$. The breathing and the spin-dipole modes are fully hybridized above the critical coupling $\Omega_{\text{cr}} \approx 2.5 E_r$, while below Ω_{cr} , a new Goldstone mode of spin nature appears. The dipole frequencies ω_D have been obtained from the center-of-mass oscillation $x_{\text{c.m.}} = \langle x \rangle$ after a sudden shift of the trap center. For $\Omega > \Omega_{\text{cr}}$, they practically coincide with the bound $\omega_x / \sqrt{1 + 2E_r \chi}$. The violation of this upper bound by ω_D for $\Omega < \Omega_{\text{cr}}$ implies the emergence of a new low-energy mode.

tial overlap [39]. Furthermore, we choose the parameters $k_0 = \sqrt{2\pi} / \lambda_{\text{Raman}}$ with $\lambda_{\text{Raman}} = 804.1 \text{ nm}$ [30], $N = 10^4$, and $\delta = 0$.

In Figs. 1(a) and 1(b), we report the time dependence of the root-mean-square radius in the x direction, $x_{\text{rms}} = \sqrt{\langle x^2 \rangle}$, and of the relative displacement of the two spin components, $d_x = \langle x \rangle_\uparrow - \langle x \rangle_\downarrow$, after the sudden removal of a static perturbation proportional to the operator x^2 , corresponding to a sudden decrease of the trapping frequency. Since the commutator $[x^2, H_{\text{SP}}]$ contains a term proportional to $x \sigma_z$, one would expect, in general, to observe two collective oscillations of hybridized density and spin nature. For values of Ω larger than the critical coupling Ω_{cr} , we instead find that the observables x_{rms} and d_x oscillate with the same frequency [see Fig. 1(b)]. This is the consequence of the locking of the relative phase of the order parameters of the two spin components characterizing the low-frequency oscillations

in the plane-wave and single-minimum phases [41].

When we enter the stripe phase, the scenario changes drastically and we observe the appearance of a new oscillation of spin nature, revealed by the beating in the signal d_x [see Fig. 1(a)]. This oscillation is the finite-size manifestation of the gapless Goldstone spin branch exhibited by the supersolid phase in uniform matter [15]. The beating reflects the fact that the two gapless branches are decoupled density and spin modes only in the limit of long wavelengths. An analogous effect has recently been identified in spin-orbit-coupled fluids of light in Kerr nonlinear media [42]. We have verified that the new mode can also be excited by applying a perturbation proportional to $x\sigma_z$, corresponding to a relative displacement of the two spin components.

In Fig. 1(c), we report the dispersion $\omega(\Omega)$ of the resulting breathing and spin-dipole excitations. The frequencies have been calculated for small perturbations in the regime of linear response, but the beating effect is clearly visible also for larger perturbation strengths [cf. Fig. 1(a)] that are closer to the onset of nonlinearities. Similar dispersion laws have been obtained in Ref. [43] by solving the Bogoliubov equations for a spin-orbit-coupled mixture in one dimension. With respect to Ref. [43], our approach explicitly exposes the beating effect between the spin-dipole excitation and the compression mode in the stripe phase, as well as the full hybridization of the two modes above Ω_{cr} .

In the limit $\Omega \rightarrow 0$, the spin-dipole frequency can be calculated analytically within the formalism of two-fluid hydrodynamics [31]. We find

$$\omega_{\text{SD}}^2(\Omega \rightarrow 0) = \omega_x^2 \frac{1 - (g_{\text{ns}}/g_{\text{ss}})^2}{g_{\text{nn}}/g_{\text{ss}} - (g_{\text{ns}}/g_{\text{ss}})^2}, \quad (3)$$

yielding the value $\omega_{\text{SD}} = 0.5\omega_x$ for the configuration considered here, in agreement with Fig. 1(c). The dispersion of the spin-dipole branch decreases as Ω approaches the transition at the critical value Ω_{cr} and is expected to vanish at the spinodal point, corresponding to a value of Ω a little higher than Ω_{cr} where the system develops a dynamic instability associated with the divergent behavior of the magnetic polarizability [44]. The decrease of ω_{SD} as a function of Ω is a crucial consequence of spin-orbit coupling and of the presence of stripes. By contrast, in the presence of radio frequency or microwave coupling, the spin-dipole frequency increases with the coupling strength, quickly approaching the value Ω of the spin gapped branch [45].

In Fig. 1(c), we also report the dispersion of the center-of-mass (dipole) mode, which is excited by suddenly removing a perturbation proportional to the operator x , corresponding to a shift of the harmonic trap along the x direction. Above Ω_{cr} , the center-of-mass operator x and the spin operator σ_z excite the same mode, similar to the case of the operators x^2 and $x\sigma_z$ discussed above. Both the breathing and the dipole frequencies decrease

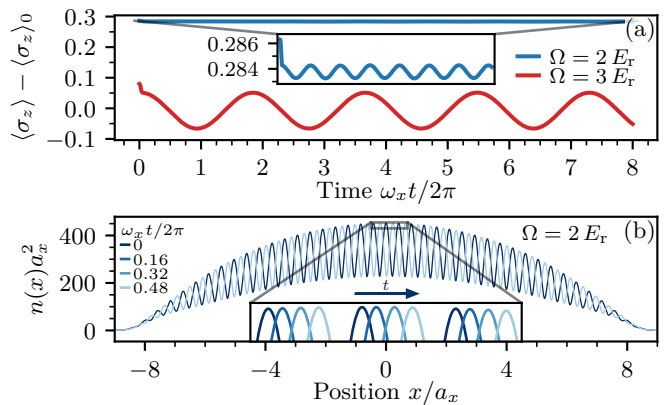


Figure 2. Evidence for the zero-frequency Goldstone mode associated with the translation of the stripes. (a) Time evolution of the polarization $\langle \sigma_z \rangle$ with respect to its equilibrium value $\langle \sigma_z \rangle_0$ after removing the perturbation $H_{\text{pert}} = -\lambda E_r \sigma_z$ with $\lambda = 0.02$ in the stripe phase ($\Omega = 2 E_r$) and $\lambda = 0.1$ in the plane-wave phase ($\Omega = 3 E_r$). In the latter case, the polarization oscillates around equilibrium at the dipole frequency $\omega_{\text{D}} \approx 0.55 \omega_x$. By contrast, in the stripe phase, the polarization remains locked for a time much longer than $2\pi/\omega_x$, providing evidence for the zero-frequency Goldstone mode. The low-amplitude oscillations at the dipole frequency $\omega_{\text{D}} \approx 0.89 \omega_x$ shown in the inset indicate a weak excitation of the center-of-mass mode. (b) Time evolution of the density profile $n(x)$ in the stripe phase for the same scenario as in (a), explicitly revealing the excitation of the translational motion of the stripes. In the linear regime, the velocity of the stripes is proportional to the perturbation strength λ according to $v(\lambda) \approx 0.48 \lambda \hbar k_0/m$.

when approaching the transition to the single-minimum phase, where the effective mass increases, inducing sizeable non-linear effects [44, 46].

At the transition to the supersolid phase, both the breathing and the dipole frequencies exhibit a small jump, reflecting the first-order nature of the supersolid–superfluid transition. Entering the supersolid phase, one expects the emergence of the Goldstone mode that corresponds, in uniform matter, to the rigid translation of stripes. In a harmonic trap, the frequency of this motion is not exactly zero, but still much smaller than the oscillator frequency ω_x . The existence of this “zero-frequency” Goldstone mode can be inferred employing a sum-rule argument, according to which a rigorous upper bound to the lowest-energy mode excited by the operator x is given by $\omega_{\text{lowest}} \leq \omega_x / \sqrt{1 + 2E_r \chi}$, where χ is the magnetic polarizability [44]. This upper bound practically coincides with the center-of-mass frequency ω_{D} if $\Omega > \Omega_{\text{cr}}$, while below Ω_{cr} the calculated value of ω_{D} violates the bound due to the large value of χ , revealing the existence of a new low-frequency mode.

To shed light on the nature of this low-energy excitation, we apply a uniform spin perturbation proportional to the operator σ_z , causing a magnetic polarization of the

system. After removing the perturbation [47], one would expect the polarization to oscillate around its equilibrium value, driven by the Raman coupling. Indeed, above Ω_{cr} , after a short initial decrease reflecting the contribution of the high-frequency gapped spin branch to the static magnetic polarizability [41], the polarization oscillates at the center-of-mass frequency [see Fig. 2(a)]. The fact that the spin operator excites the center-of-mass mode is a manifestation of the hybridization mechanism between the operators x and σ_z , similar to the one discussed above for x^2 and $x\sigma_z$.

In the stripe phase, we find instead that the polarization remains locked to its initial value throughout the simulation time, with a residual small-amplitude oscillation stemming from a weak excitation of the center-of-mass mode by the spin operator σ_z . We have verified that the locking of the polarization survives longer than 1000 times the oscillator time $2\pi/\omega_x$, confirming the anticipated low frequency of the Goldstone mode. Remarkably, releasing the spin perturbation has the effect of applying a boost to the stripes, causing their translation at a constant velocity proportional to the perturbation strength, as illustrated in Fig. 2(b). The translation of the stripes is practically independent of the center-of-mass motion, thereby providing direct evidence for the excitation of the zero-frequency Goldstone mode. By contrast, after suddenly shifting the trap center, corresponding to a perturbation by the dipole operator x , the center of mass oscillates around equilibrium both in the superfluid and in the supersolid phase (not shown). This shows that the zero-frequency Goldstone mode contributes only marginally to the static dipole polarizability, whereas its strong excitation by the operator σ_z implies that it constitutes the predominant contribution to the magnetic polarizability in the stripe phase.

In the last part of this Letter, we focus on a configuration characterized by strongly asymmetric intraspecies interactions, $g_{\uparrow\uparrow} \gg g_{\downarrow\downarrow} \approx g_{\uparrow\downarrow}$, yielding $g_{\text{nn}} \approx g_{\text{ss}} \approx g_{\text{ns}}$. The main motivation is to explore the consequences of the high spin polarization on the stripe phase, relevant for the case of ^{39}K , which has recently become available for experiments on spin-orbit-coupled Bose-Einstein condensates [48]. We consider a set of scattering lengths given by $a_{\uparrow\uparrow} = 252.7 a_0$, $a_{\downarrow\downarrow} = 1.3 a_0$, and $a_{\uparrow\downarrow} = -6.3 a_0$, realizable in ^{39}K by using Feshbach resonances near a magnetic field of $B \approx 389 \text{ G}$ [48]. These values are consistent with the stability condition $g_{\uparrow\uparrow}g_{\downarrow\downarrow} > g_{\uparrow\downarrow}^2$. Furthermore, we choose $k_0 = 2\pi/\lambda_{\text{Raman}}$ with $\lambda_{\text{Raman}} = 768.97 \text{ nm}$ [48], $(\omega_x, \omega_y, \omega_z) = 2\pi \times (50, 200, 200) \text{ Hz}$, $N = 10^5$, and $\delta = 0$. With these parameters, the transition to the supersolid phase occurs at $\Omega_{\text{cr}} \approx 1.0 E_r$, leading to fringes with high contrast and hence to observable supersolid effects.

Because of the strong asymmetry in the interspecies interactions ($g_{\uparrow\uparrow}/g_{\downarrow\downarrow} \approx 194$), energetic minimization favors a large value of the spin polarization. In particular, the polarization is large also in the stripe phase, as op-

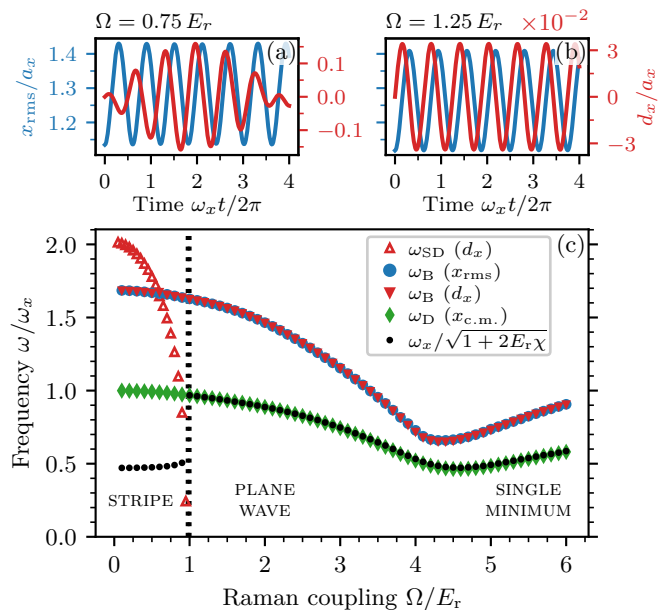


Figure 3. Same as Fig. 1, but for strongly asymmetric intraspecies interactions, as relevant for ^{39}K . The asymmetry leads to a smooth crossover between the plane-wave and the single-minimum regime. Nevertheless, in the stripe phase, the beating effects (a) and the additional frequencies (c) characteristic of the Goldstone mode are evident, while they are absent in the plane-wave phase (b).

posed to the symmetric case, where it instead vanishes. A simple estimate of this effect can be obtained in uniform matter, where, for $\Omega \rightarrow 0$, the variation of the energy (2) yields the expression $s_z/n = -g_{\text{ns}}/g_{\text{ss}}$, which amounts to a polarization of $\langle \sigma_z \rangle \approx -0.94$ for our parameters. An important consequence of the strong asymmetry of the intraspecies interactions is that the central density, dominated by the majority component Ψ_{\downarrow} , is strongly enhanced with respect to the usual values characterizing symmetric configurations. This effect is accompanied by a shrinking of the cloud radius and the occurrence of fringes with high contrast in the minority component Ψ_{\uparrow} .

Following the procedure employed in the symmetric case, we consider the relative displacement d_x of the two components after a sudden quench of the trapping frequency [see Figs. 3(a) and 3(b)]. Also in this case, we observe a clear beating effect, revealing the occurrence of a Goldstone mode of spin nature in the stripe phase. Because of the large polarization of the system, this mode mainly corresponds to the motion of the minority component, while the majority component remains practically at rest.

In Fig. 3(c), we show the dispersion law of the resulting elementary excitations as a function of Ω , along with the dispersion of the center-of-mass mode excited by shifting the trap center. At $\Omega \rightarrow 0$, the spin-dipole frequency is larger than the center-of-mass frequency as a result of the negative interspecies interaction $g_{\uparrow\downarrow}$, in agreement with

Eq. (3). Because of the asymmetry of the intraspecies interactions, the transition between the plane-wave and the single-minimum phase is less sharp than in the symmetric case and actually becomes a smooth crossover. Furthermore, we find that the contrast of the stripes does not exhibit a jump at the supersolid–superfluid transition, but vanishes continuously, which may indicate that, due to the smallness of $g_{\downarrow\downarrow}$, the system is still rather far from the thermodynamic limit. Nonetheless, the qualitative features of the excitation spectrum, including the occurrence of the zero-frequency Goldstone mode, are similar to the symmetric case.

In conclusion, we have provided accessible signatures of the Goldstone modes exhibited by the stripe phase of a harmonically trapped spin–orbit-coupled Bose–Einstein condensate. The Goldstone modes are revealed by a characteristic beating effect in the spin-dipole observable, following an experimentally straightforward density perturbation, and by the dynamic excitation of the translational motion of the stripes (zero-frequency Goldstone mode), following the release of a uniform spin perturbation. Both configurations with symmetric and highly asymmetric intraspecies interactions provide promising platforms for observing these effects. Our results illustrate the rich hybridization phenomena that appear in a supersolid system with non-trivial spin degree of freedom and how these open new routes to identifying fundamental hallmarks of supersolidity.

We thank Li Chen, Han Pu, Jean Dalibard, Gabriele Ferrari, and the ICFO team led by Leticia Tarruell for fruitful discussions. This project has received funding from the European Research Council (ERC) under the European Union’s Horizon 2020 research and innovation programme (ERC StG StrEnQTh, Grant Agreement No. 804305), the Provincia Autonoma di Trento, and Q@TN — Quantum Science and Technology in Trento. The authors acknowledge support by the state of Baden-Württemberg through bwHPC.

* kevinthomas.geier@unitn.it

- [1] D. J. Thouless, The flow of a dense superfluid, *Ann. Phys. (N.Y.)* **52**, 403 (1969).
- [2] A. F. Andreev and I. M. Lifshitz, Quantum theory of defects in crystals, *Zh. Eksp. Teor. Fiz.* **56**, 2057 (1969), [*Sov. Phys. JETP* **29**, 1107 (1969)].
- [3] A. J. Leggett, Can a solid be “superfluid”?, *Phys. Rev. Lett.* **25**, 1543 (1970).
- [4] S. Balibar, The enigma of supersolidity, *Nature (London)* **464**, 176 (2010).
- [5] M. Boninsegni and N. V. Prokof’ev, Colloquium: Supersolids: What and where are they?, *Rev. Mod. Phys.* **84**, 759 (2012), [arXiv:1201.2227](https://arxiv.org/abs/1201.2227) [*cond-mat.stat-mech*].
- [6] J. Léonard, A. Morales, P. Zupancic, T. Esslinger, and T. Donner, Supersolid formation in a quantum gas breaking a continuous translational symmetry, *Nature (London)* **543**, 87 (2017), [arXiv:1609.09053](https://arxiv.org/abs/1609.09053) [*cond-mat.quant-gas*].
- [7] J.-R. Li, J. Lee, W. Huang, S. Burchesky, B. Shteynas, F. Ç. Top, A. O. Jamison, and W. Ketterle, A stripe phase with supersolid properties in spin–orbit-coupled Bose–Einstein condensates, *Nature (London)* **543**, 91 (2017), [arXiv:1610.08194](https://arxiv.org/abs/1610.08194) [*cond-mat.quant-gas*].
- [8] A. Putra, F. Salces-Cárcoba, Y. Yue, S. Sugawa, and I. B. Spielman, Spatial coherence of spin–orbit-coupled Bose gases, *Phys. Rev. Lett.* **124**, 053605 (2020), [arXiv:1910.03613](https://arxiv.org/abs/1910.03613) [*cond-mat.quant-gas*].
- [9] L. Tanzi, E. Lucioni, F. Famà, J. Catani, A. Fioretti, C. Gabbanini, R. N. Bisset, L. Santos, and G. Modugno, Observation of a dipolar quantum gas with metastable supersolid properties, *Phys. Rev. Lett.* **122**, 130405 (2019), [arXiv:1811.02613](https://arxiv.org/abs/1811.02613) [*cond-mat.quant-gas*].
- [10] F. Böttcher, J.-N. Schmidt, M. Wenzel, J. Hertkorn, M. Guo, T. Langen, and T. Pfau, Transient supersolid properties in an array of dipolar quantum droplets, *Phys. Rev. X* **9**, 011051 (2019), [arXiv:1901.07982](https://arxiv.org/abs/1901.07982) [*cond-mat.quant-gas*].
- [11] L. Chomaz, D. Petter, P. Ilzhöfer, G. Natale, A. Trautmann, C. Politi, G. Durastante, R. M. W. van Bijnen, A. Patscheider, M. Sohmen, M. J. Mark, and F. Ferlaino, Long-lived and transient supersolid behaviors in dipolar quantum gases, *Phys. Rev. X* **9**, 021012 (2019), [arXiv:1903.04375](https://arxiv.org/abs/1903.04375) [*cond-mat.quant-gas*].
- [12] C. Josseland, Y. Pomeau, and S. Rica, Patterns and supersolids, *Eur. Phys. J. Spec. Top.* **146**, 47 (2007).
- [13] S. Sacconi, S. Moroni, and M. Boninsegni, Excitation spectrum of a supersolid, *Phys. Rev. Lett.* **108**, 175301 (2012), [arXiv:1201.4784](https://arxiv.org/abs/1201.4784) [*cond-mat.quant-gas*].
- [14] M. Kunimi and Y. Kato, Mean-field and stability analyses of two-dimensional flowing soft-core bosons modeling a supersolid, *Phys. Rev. B* **86**, 060510(R) (2012), [arXiv:1205.2126](https://arxiv.org/abs/1205.2126) [*cond-mat.quant-gas*].
- [15] Y. Li, G. I. Martone, L. P. Pitaevskii, and S. Stringari, Superstripes and the excitation spectrum of a spin–orbit-coupled Bose–Einstein condensate, *Phys. Rev. Lett.* **110**, 235302 (2013), [arXiv:1303.6903](https://arxiv.org/abs/1303.6903) [*cond-mat.quant-gas*].
- [16] T. Macri, F. Maucher, F. Cinti, and T. Pohl, Elementary excitations of ultracold soft-core bosons across the superfluid–supersolid phase transition, *Phys. Rev. A* **87**, 061602(R) (2013), [arXiv:1212.6934](https://arxiv.org/abs/1212.6934) [*cond-mat.quant-gas*].
- [17] R. Liao, Searching for supersolidity in ultracold atomic Bose condensates with Rashba spin–orbit coupling, *Phys. Rev. Lett.* **120**, 140403 (2018), [arXiv:1804.01163](https://arxiv.org/abs/1804.01163) [*cond-mat.quant-gas*].
- [18] S. M. Rocuzzo and F. Ancilotto, Supersolid behavior of a dipolar Bose–Einstein condensate confined in a tube, *Phys. Rev. A* **99**, 041601(R) (2019), [arXiv:1810.12229](https://arxiv.org/abs/1810.12229) [*cond-mat.quant-gas*].
- [19] H. Lyu and Y. Zhang, Spin–orbit-coupling-assisted roton softening and superstripes in a Rydberg-dressed Bose–Einstein condensate, *Phys. Rev. A* **102**, 023327 (2020), [arXiv:2003.10090](https://arxiv.org/abs/2003.10090) [*cond-mat.quant-gas*].
- [20] G. I. Martone, A. Recati, and N. Pavloff, Supersolidity of cnoidal waves in an ultracold Bose gas, *Phys. Rev. Research* **3**, 013143 (2021), [arXiv:2008.00795](https://arxiv.org/abs/2008.00795) [*cond-mat.quant-gas*].
- [21] J. Hofmann and W. Zwerger, Hydrodynamics of a superfluid smectic, *J. Stat. Mech. Theory Exp.* **2021**, 033104 (2021), [arXiv:2012.06569](https://arxiv.org/abs/2012.06569) [*cond-mat.quant-gas*].

- [22] J. Léonard, A. Morales, P. Zupancic, T. Donner, and T. Esslinger, Monitoring and manipulating Higgs and Goldstone modes in a supersolid quantum gas, *Science* **358**, 1415 (2017), [arXiv:1704.05803 \[cond-mat.quant-gas\]](#).
- [23] L. Tanzi, S. M. Roccuzzo, E. Lucioni, F. Famà, A. Fioretti, C. Gabbanini, G. Modugno, A. Recati, and S. Stringari, Supersolid symmetry breaking from compressional oscillations in a dipolar quantum gas, *Nature (London)* **574**, 382 (2019), [arXiv:1906.02791 \[cond-mat.quant-gas\]](#).
- [24] M. Guo, F. Böttcher, J. Hertkorn, J.-N. Schmidt, M. Wenzel, H. P. Büchler, T. Langen, and T. Pfau, The low-energy Goldstone mode in a trapped dipolar supersolid, *Nature (London)* **574**, 386 (2019), [arXiv:1906.04633 \[cond-mat.quant-gas\]](#).
- [25] G. Natale, R. M. W. van Bijnen, A. Patscheider, D. Petter, M. J. Mark, L. Chomaz, and F. Ferlaino, Excitation spectrum of a trapped dipolar supersolid and its experimental evidence, *Phys. Rev. Lett.* **123**, 050402 (2019), [arXiv:1907.01986 \[cond-mat.quant-gas\]](#).
- [26] D. Petter, A. Patscheider, G. Natale, M. J. Mark, M. A. Baranov, R. van Bijnen, S. M. Roccuzzo, A. Recati, B. Blakie, D. Baillie, L. Chomaz, and F. Ferlaino, Bragg scattering of an ultracold dipolar gas across the phase transition from Bose–Einstein condensate to supersolid in the free-particle regime, *Phys. Rev. A* **104**, L011302 (2021), [arXiv:2005.02213 \[cond-mat.quant-gas\]](#).
- [27] J. Dalibard, F. Gerbier, G. Juzeliūnas, and P. Öhberg, Colloquium: Artificial gauge potentials for neutral atoms, *Rev. Mod. Phys.* **83**, 1523 (2011), [arXiv:1008.5378 \[cond-mat.quant-gas\]](#).
- [28] V. Galitski and I. B. Spielman, Spin–orbit coupling in quantum gases, *Nature (London)* **494**, 49 (2013), [arXiv:1312.3292 \[cond-mat.quant-gas\]](#).
- [29] M. Aidelsburger, S. Nascimbene, and N. Goldman, Artificial gauge fields in materials and engineered systems, *C. R. Phys.* **19**, 394 (2018), [arXiv:1710.00851 \[cond-mat.mes-hall\]](#).
- [30] Y.-J. Lin, K. Jiménez-García, and I. B. Spielman, Spin–orbit-coupled Bose–Einstein condensates, *Nature (London)* **471**, 83 (2011), [arXiv:1103.3522 \[cond-mat.quant-gas\]](#).
- [31] L. P. Pitaevskii and S. Stringari, *Bose–Einstein Condensation and Superfluidity*, 1st ed., International Series of Monographs on Physics, Vol. 164 (Oxford University Press, Oxford, United Kingdom, 2016).
- [32] Y. Li, G. I. Martone, and S. Stringari, Spin–orbit-coupled Bose–Einstein condensates, in *Annual Review of Cold Atoms and Molecules*, Vol. 3, edited by K. W. Madison, K. Bongs, L. D. Carr, A. M. Rey, and H. Zhai (World Scientific, Singapore, 2015) Chap. 5, pp. 201–250, [arXiv:1410.5526 \[cond-mat.quant-gas\]](#).
- [33] W. Zheng, Z.-Q. Yu, X. Cui, and H. Zhai, Properties of Bose gases with the Raman-induced spin–orbit coupling, *J. Phys. B* **46**, 134007 (2013), [arXiv:1212.6832 \[cond-mat.quant-gas\]](#).
- [34] X.-L. Chen, J. Wang, Y. Li, X.-J. Liu, and H. Hu, Quantum depletion and superfluid density of a supersolid in Raman spin–orbit-coupled Bose gases, *Phys. Rev. A* **98**, 013614 (2018), [arXiv:1805.02320 \[cond-mat.quant-gas\]](#).
- [35] X. Antoine, A. Levitt, and Q. Tang, Efficient spectral computation of the stationary states of rotating Bose–Einstein condensates by preconditioned non-linear conjugate gradient methods, *J. Comput. Phys.* **343**, 92 (2017), [arXiv:1611.02045 \[math.NA\]](#).
- [36] X. Antoine, W. Bao, and C. Besse, Computational methods for the dynamics of the non-linear Schrödinger/Gross–Pitaevskii equations, *Comput. Phys. Commun.* **184**, 2621 (2013), [arXiv:1305.1093 \[math.NA\]](#).
- [37] T.-L. Ho and S. Zhang, Bose–Einstein condensates with spin–orbit interaction, *Phys. Rev. Lett.* **107**, 150403 (2011).
- [38] Y. Li, L. P. Pitaevskii, and S. Stringari, Quantum tricriticality and phase transitions in spin–orbit-coupled Bose–Einstein condensates, *Phys. Rev. Lett.* **108**, 225301 (2012), [arXiv:1202.3036 \[cond-mat.quant-gas\]](#).
- [39] G. I. Martone, Y. Li, and S. Stringari, Approach for making visible and stable stripes in a spin–orbit-coupled Bose–Einstein superfluid, *Phys. Rev. A* **90**, 041604(R) (2014), [arXiv:1409.3149 \[cond-mat.quant-gas\]](#).
- [40] G. I. Martone, Visibility and stability of superstripes in a spin–orbit-coupled Bose–Einstein condensate, *Eur. Phys. J. Special Topics* **224**, 553 (2015), [arXiv:1505.02088 \[cond-mat.quant-gas\]](#).
- [41] G. I. Martone, Y. Li, L. P. Pitaevskii, and S. Stringari, Anisotropic dynamics of a spin–orbit-coupled Bose–Einstein condensate, *Phys. Rev. A* **86**, 063621 (2012), [arXiv:1207.6804 \[cond-mat.quant-gas\]](#).
- [42] G. I. Martone, T. Bienaimé, and N. Cherroret, Spin–orbit-coupled fluids of light in bulk non-linear media, *Phys. Rev. A* **104**, 013510 (2021), [arXiv:2104.11982 \[physics.optics\]](#).
- [43] L. Chen, H. Pu, Z.-Q. Yu, and Y. Zhang, Collective excitation of a trapped Bose–Einstein condensate with spin–orbit coupling, *Phys. Rev. A* **95**, 033616 (2017), [arXiv:1704.01242 \[cond-mat.quant-gas\]](#).
- [44] Y. Li, G. I. Martone, and S. Stringari, Sum rules, dipole oscillation and spin polarizability of a spin–orbit-coupled quantum gas, *Europhys. Lett.* **99**, 56008 (2012), [arXiv:1205.6398 \[cond-mat.quant-gas\]](#).
- [45] A. Sartori, J. Marino, S. Stringari, and A. Recati, Spin-dipole oscillation and relaxation of coherently coupled Bose–Einstein condensates, *New J. Phys.* **17**, 093036 (2015), [arXiv:1503.05000 \[cond-mat.quant-gas\]](#).
- [46] J.-Y. Zhang, S.-C. Ji, Z. Chen, L. Zhang, Z.-D. Du, B. Yan, G.-S. Pan, B. Zhao, Y.-J. Deng, H. Zhai, S. Chen, and J.-W. Pan, Collective dipole oscillations of a spin–orbit-coupled Bose–Einstein condensate, *Phys. Rev. Lett.* **109**, 115301 (2012), [arXiv:1201.6018 \[cond-mat.quant-gas\]](#).
- [47] To avoid the excitation of high-frequency modes on the order of the Raman coupling, we switch off the perturbation smoothly within a time interval τ chosen such that $2\pi\hbar/\Omega \ll \tau \ll 2\pi/\omega_x$.
- [48] L. Tarruell, Private communication (2020).